

# Novel Method for *In-situ* and Simultaneous Nano-friction and Nano-wear Characterization of Materials

Running title: Novel Nanotribological Method

Running Authors: Broitman and Florez-Ruiz

Esteban Broitman <sup>a), b)</sup>

Thin Film Physics Division, IFM, Linköping University, SE-581-83 Linköping, Sweden

F. J. Flores-Ruiz

Centro de Investigación y de Estudios Avanzados del I.P.N., Unidad Querétaro. Qro 76230, México

<sup>a)</sup>American Vacuum Society member.

<sup>b)</sup>Electronic mail: [esbro@ifm.liu.se](mailto:esbro@ifm.liu.se)

## Abstract

*Nowadays there is an increased need to know the nanotribological properties of protective coatings used in part devices operating under nano- and micro-contact situations, e.g. hard disk drives, magnetic heads, micro-electromechanical systems (MEMS) and microsensors, etc. Therefore there is a demand for instruments and methods testing friction and wear at the nano- and micro-scales.*

*In this work we present a new methodology to measure simultaneously the friction, and wear of a surface. We have designed an experiment where a probe is permanently scanning a 10  $\mu\text{m}$  track in a reciprocal movement. Different loads are applied in order to obtain the topographic information which is used to calculate the wear rate and roughness evolution. Force lateral sensors register simultaneously the friction force variations. The*

*experimental input data are information vectors that contain: load ( $\mu\text{N}$ ), friction force ( $\mu\text{N}$ ), vertical Z displacement (nm), lateral X displacement (nm) and time (s). The data is processed using a simple program running in MathLab® which eliminates the thermal drift. The software output gives the resulting friction coefficient, track roughness, and wear rate as a function of the running cycles of the probe. The new method builds a novel bridge to relate tribological mechanisms at different scales.*

## **I. INTRODUCTION**

During the last two decades, the tribological characterization of coated surfaces at the micro- and nano-scales has become of increasing importance in many technological applications where coatings in the range of some tens to hundreds of nanometers thickness are used. Therefore, there is a need not only for new and more precise instruments but also for new testing methods<sup>1,2</sup>.

The earlier nanotribological methods have been based on atomic force microscopes (AFMs). A tip with an apex radius of about 50 nm, usually made of  $\text{Si}_3\text{N}_4$ , was moved over the surface with a high applied load,  $\sim 100$  nN, to create wear marks on the surface than later were imaged using the same tip at a low load ( $\sim 10$  nN)<sup>3</sup>. The first experiments have allowed the researchers to characterize ultra-thin diamond-like carbon (DLC) coatings deposited on hard disks and magnetic recording heads, and also to carry out basic research on the origin of friction and wear at the atomic and molecular scale. Friction characterization with AFM has also been done in some cases where a careful calibration of the instrument allowed the recording of static and dynamic friction over dry and lubricated surfaces<sup>4</sup>.

The development of micro electro-mechanical systems (MEMS) brought an interest in small machines, whose tribological characterization has been carried out usually by the design of dedicated MEMS devices. Furthermore, the use of MEMS and the developing of electrostatic force transducer systems during the last decade have given place to new instruments allowing the precise nanoscale determination of vertical loads, lateral forces, and 3D displacements.

Traditionally, the measurement of wear at the micro- and nano-scale is carried out by two methods<sup>4</sup>:

- i) a two-dimensional test where the tip scans the surface while a relatively high normal load is applied to it. The tip produces a squared hole, whose volume can be measured when the experiment has finished by comparing the initial and final surface topography. There is drawback in this method because, given a fixed size of the tip, the wear rate will depend not only on the load, but also on the number of scanned lines per frame<sup>5</sup>. Furthermore, the tip is also under high tribological wear process during the experiment, especially when analyzing hard and abrasive surfaces, leading to uncontrolled dynamic changes of contact pressure between the probe and surface.

- ii) a linear oscillating test where the tip moves a certain number of cycles at a fix high load, giving as a result the production of a trench. This method presents an advantage regarding tip wear because the area under analysis is substantially smaller.

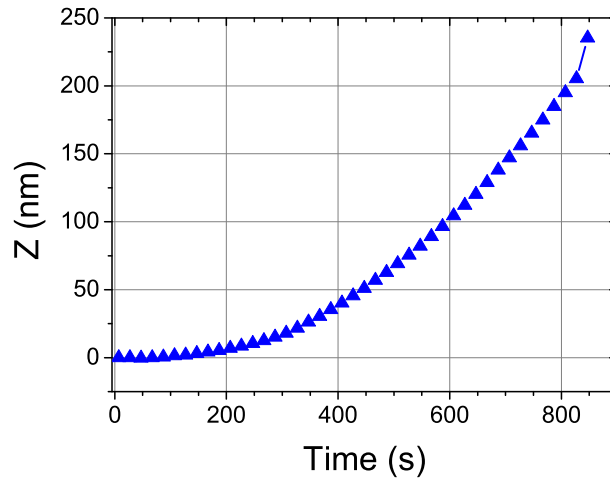


FIG. 1. (Color Online) The vertical position  $Z$  of a conical diamond tip oscillating at 0.05 Hz on a fused-silica surface with an applied load of  $2 \mu\text{N}$ . The amplitude of the reciprocating movement is  $10 \mu\text{m}$  and the applied load is  $2 \mu\text{N}$ . The tip thermal drift was corrected at  $t = 0 \text{ s}$ .

There have been some publications trying to calculate the progression of the wear rate using linear oscillation tests<sup>5-7</sup>. However, all of them have ignored the presence of thermal drift (TD) during the experiments. Most of commercial systems have software with a routine to evaluate the TD before an experiment is carried out: it is usually measured over a time lapse of 30-90 seconds, and then the software assumes that the drift is constant during the rest of the experiment. This assumption is reasonable on experiments of few seconds duration (like in a nanoindentation). However, given its random nature, is difficult to predict the drift evolution on experiments of many minutes duration. Figure 1 illustrates an example of the drift measured when a tip is dragged in a 0.05 Hz oscillating movement of  $10 \mu\text{m}$  length over a hard and smooth fused-silica surface with an applied load of  $2 \mu\text{N}$  during 850 seconds. If there were no drift, the vertical position  $Z$  of the tip should be

constant. However, due to TD, it is observed that the tip drifts with a non-constant drift rate.

In this paper, we have designed an experiment for a linear oscillating tribological test which eliminates the problem of TD, giving *in-situ* and simultaneously the evolution of friction and wear in each cycle. Results obtained from a graphite sample are presented under dry and lubricated experiments to demonstrate the power of our technique which allows a precise calculation of tribological properties at the nanoscale.

## II. EXPERIMENTAL

All the experiments were done using a Triboindenter TI-950 from Hysitron. The Triboindenter is a commercial system whose primary function is nanoindentation. The heart of the instrument is a three-plate capacitive transducer assembly that is used as both, the actuator and sensor of the instrument<sup>8</sup>. The force on a tip mounted in the center plate of a capacitor is applied electrostatically while the displacement is simultaneously measured by the change in capacitance. This capacitive transducer assembly is mounted to a three-axis piezo tube-scanner similar to those found in AFMs. The tube-scanner scans the sample while the indenter tip is maintained in contact at constant load with a surface. Under these conditions, the transducer collects z displacement data and produces AFM-like images. The system also allows applying not only low forces for imaging ( $\sim 2 \mu\text{N}$ ) but also high forces of up to 12 mN while measuring friction forces. All system is computer-controlled, with all the components mounted on a granite table over an active vibration isolation device to dampen vibrational effects, and enclosed in a thermal-acoustical isolation chamber<sup>8</sup>.

The instrument presents many advantages for the measurement of friction and wear at the nanoscale. A reciprocating multi-cycle linear test can be programmed, from where it

is possible to obtain simultaneously the friction force and wear rate from the lateral force and vertical displacement sensors, respectively. The friction values have high precision but the wear data given by the software is usually wrong in long duration experiments because of the thermal drift rate. In comparison to electromagnetic sensors of other commercial systems, the electrostatic actuation of the Triboindenter requires very little current which produces a low thermal drift of  $\sim 0.05 \text{ nm/s}^8$ . Furthermore, the software includes a preliminary thermal drift correction before each measurement which usually measures the drift during 30 s and compensates the following measurement assuming a constant drift rate during the experiment. This assumption is usually good enough for a nanoindentation of  $\sim 10 \text{ s}$  duration, but in wear experiments of more than 100 s, a drift rate of just  $0.05 \text{ nm/s}$  can lead to big wear errors, as we show in Figure 1. We have designed a special experiment and developed a data processing program to eliminate the thermal drift problem, as described in the next section.

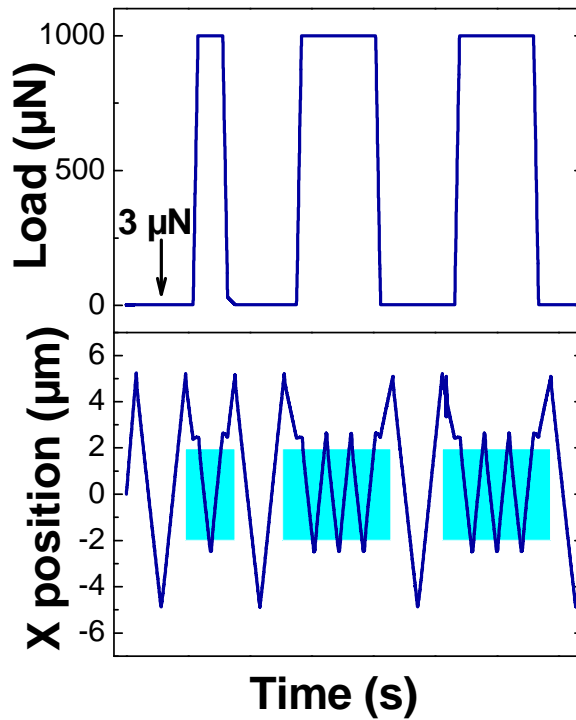


FIG. 2. (Color Online) Experimental profile used to obtain the in-situ and simultaneous tribological

### III. Measurement Procedures

#### A. Profile for friction and wear tests

The profile designed to obtain the tribological characteristics of the materials is shown in figure 2. The upper plot shows the load profile applied on the z axis (normal to the surface) as a function of time, consisting of: a) the base-load ( $3 \mu\text{N}$ ) used to obtain the topographic profile and b) a high load used to produce wear and measure friction. The bottom image in figure 2 illustrates the position of the tip on the surface as a function of time. With this experimental setup, schematically illustrated in figure 3, is possible to

obtain topography, coefficient of friction, roughness, and wear rate *in-situ* and simultaneously in the same experiment.

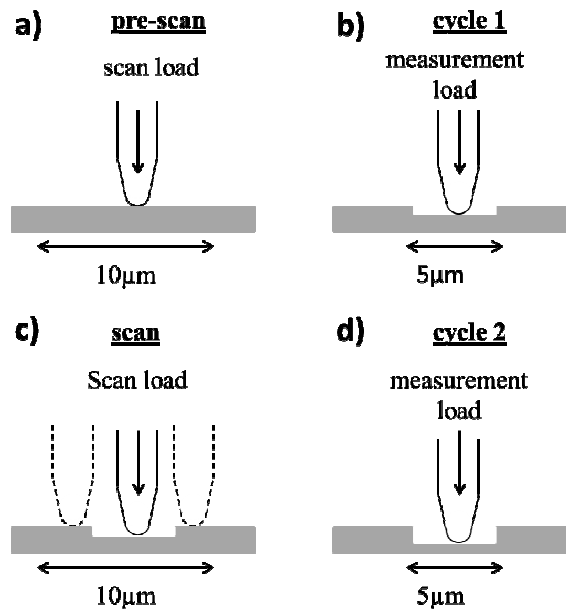


FIG. 3. Schematics of the method: (a) pre-scan to get the topographical profile; (b) first cycle of wear; (c) post-scan to get the new topographical profile; (d) second cycle of wear. The process repeats 10 times.

In the beginning of the experiment, two passes of  $10\mu\text{m}$  length are made in order to obtain topographic profiles with an applied load of  $3\mu\text{N}$  (fig 3a). The topography will be used to characterize the surface before the wear experiment. Then, the load is increased to the desired value ( $10\mu\text{N}$ ,  $100\mu\text{N}$ , and  $1000\mu\text{N}$  in the present experiments) at  $x = 2.5\mu\text{m}$ , and the first cycle of wear starts with two passes that we call “*trace*” and “*retrace*” (forward and backward) from  $x = 2.5\mu\text{m}$  to  $x = -2.5\mu\text{m}$  ( $5\mu\text{m}$  length) as illustrated in figure 3b. After the first cycle of friction and wear measurement finishes, the base load is



decreased again to 3  $\mu\text{N}$ , and the length of the passes are extended from  $x = 5 \mu\text{m}$  to  $x = -5 \mu\text{m}$  (10  $\mu\text{m}$  length) to explore the effects of the first wear cycle on the topography (figure 3c). After this first track scan, the load increases again (fig. 3 d) and three cycles at high load are made (three traces and three retraces), then the load is removed and two profiles of the topography are obtained. This process of three cycles at high load and two scans at 3  $\mu\text{N}$  is repeated ten times.

The experimental data obtained from the profiles shown in figure 2 are information vectors that contain: load ( $\mu\text{N}$ ), friction force ( $\mu\text{N}$ ), Z displacement (nm), X displacement (nm) and time (s). The data is processed using a simple program running in MathLab<sup>®</sup>. In order to eliminate the drift rate, the program compares all the topographical profiles taken after the first wear cycle and subsequently every three wear cycles, and automatically matches them with the profile taken before the experiments in the regions where there is no wear:  $0 < X < 2.5 \mu\text{m}$  and  $7.5 < X < 10.0 \mu\text{m}$ . In this way, all the thermal drift occurring during the wear cycles is eliminated. Figure 4 illustrates the program procedure for one topographical profile taken after the tribological test. The program works optimizing the superposition through a minimization of the difference in the vertical position between original and after-test profiles.

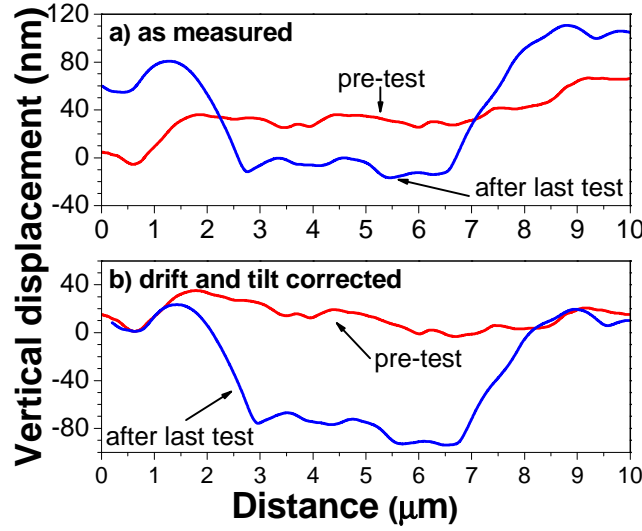


FIG. 4. (Color Online) Example of drift and tilt correction: (a) The profiles taken before (red) and after (blue) the tribological test. The measured profiles are tilted and also the profile taken after the test is vertically displaced in relation to the one taken before the test. (b) The program corrects the tilting of the profiles, and superpose them in the areas where no tribological tests have taken place ( $0 < X < 2.5 \mu\text{m}$  and  $7.5 < X < 10.0 \mu\text{m}$ ).

### **B. Coefficient of friction (CoF)**

The friction force ( $F_F$ ) is obtained as the mean value of the recorded friction forces in the shadowed blue zones of the figure 2 between  $-2 \mu\text{m}$  and  $2 \mu\text{m}$ , in trace and retrace. We don't take the full wear track to avoid “border effects” due to the accumulation of material as a result of the wear. Also, we take the mean value in trace and retrace to eliminate any effect due to an inclination of the surface, in the same way that is done for AFMs<sup>4</sup>. The coefficient of friction  $\mu$  is then obtained considering that the friction force is directly proportional to the applied load ( $L$ ), with a constant proportionality  $\mu^l$ :

$$\mu = \frac{F_F}{L} \quad (1)$$

### **C. Trench Roughness**

The average trench roughness ( $R_a$ ) is obtained from the topography profiles in the wear track during the experiments using the equation:

$$R_a = \frac{1}{N} \sum_{j=1}^N |z_j - \bar{z}| \quad (2)$$

The relative roughness (in %), calculated as  $100 \times R_a / R_0$  where  $R_0$  is the roughness of the track before the first experiment, gives an idea about the percentage of roughness increase or decrease. This information is particularly useful when comparing samples of different initial roughness.

#### **D. Wear ratio and wear rate**

The wear ratio ( $\text{nm}^2$ ) is handled as the difference in area of the first profile (topography no altered by wear) and the profiles of topography after each cycle in the wear track. Although the length of the wear track is  $5 \mu\text{m}$ , only data within  $4 \mu\text{m}$  central blue zone in figure 2 were used to evaluate the wear.

The program also computes the wear rate ( $\text{mm}^3\text{N}^{-1}\text{m}^{-1}$ ), which is simply the wear volume divided by the product of the normal load and the sliding distance. The wear volume is estimated considering the projected area  $A$  of the tip as a function of the penetration depth ( $h$ ),  $A = \pi(2Rh - h^2)$ , where  $R$  is the tip radius. The volume of the displaced material during each cycle is calculated as the sum of areas at the different penetration depths of the track. Another important data are the load applied (10, 100 and 1000  $\mu\text{N}$  used in this paper) and the length of the wear-track ( $-2 \mu\text{m} < x < 2 \mu\text{m}$ ).

## IV. Experimental Example

A carbon (graphite) sample of 20 x 20 x 6 mm, cut from a C sputtering target manufactured by K.J. Lesker was chosen as test material. A 90° conical diamond indenter with a tip end of 5.06 μm diameter was used for the friction and wear tests, with applied loads of 10, 100, and 1000 μN. All experiments were done at room temperature (22 °C), with dry tests at laboratory humidity conditions (50 %), and wet experiments with distilled water used as lubricant.

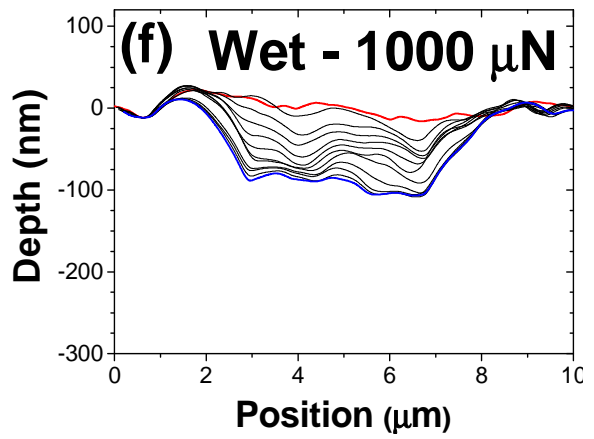
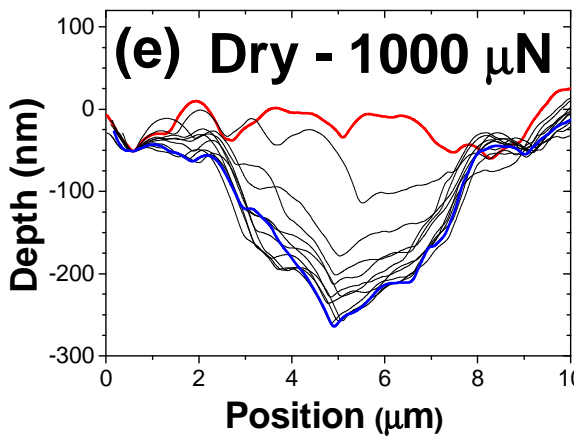
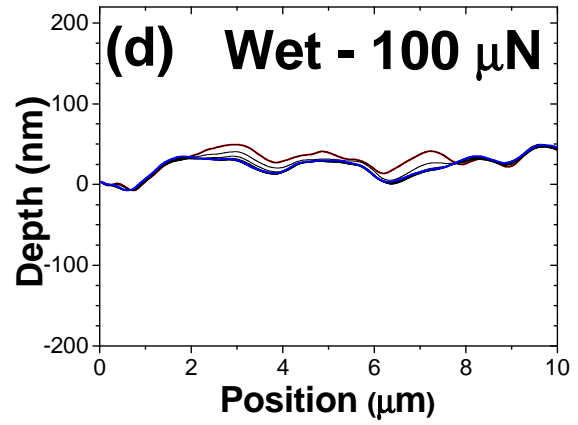
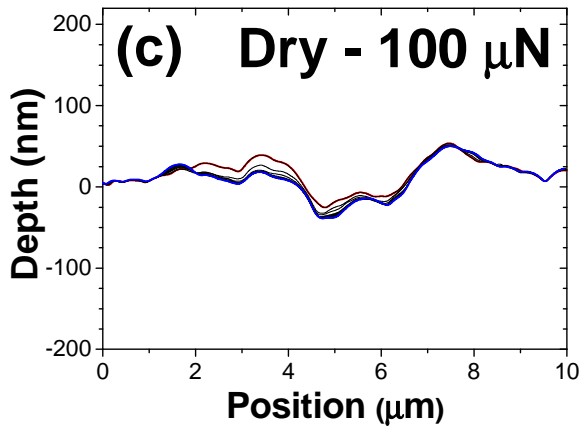
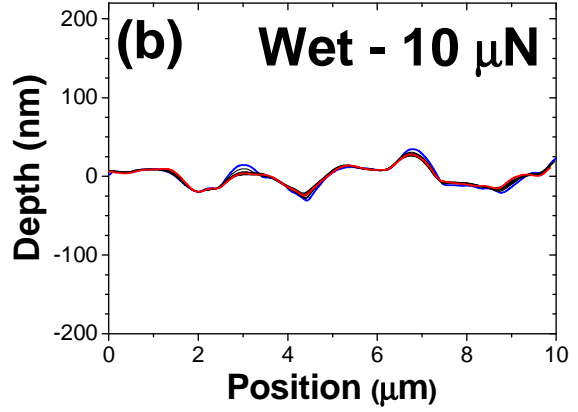
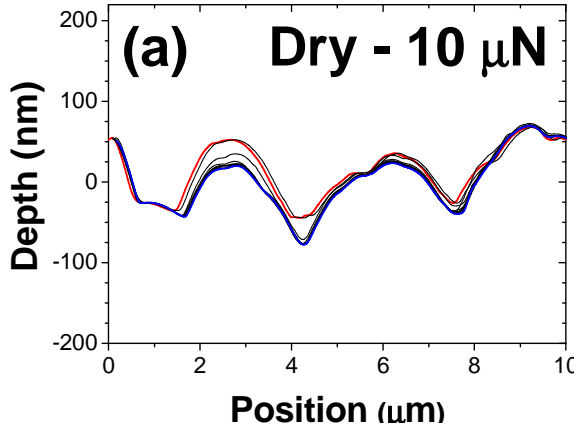


FIG.5. (Color Online) Profiles obtained simultaneously during the tribological test for a carbon sample. The virgin surface is the red line while the blue line is the profile after the last cycle. The thin black lines illustrate the evolution of the topographical profile with the different cycles. The figures in the left column (a, c, e) correspond to dry friction experiments, and the ones in the right (b, d, f) are from tests with water lubrication. The applied loads were 10  $\mu\text{N}$  (a, b); 100  $\mu\text{N}$  (c, d); and 1000  $\mu\text{N}$  (e, f).

Figure 5 shows the wear profiles obtained for three different load conditions in dry and wet conditions. It is observed that at each applied load, the profiles obtained in dry conditions (fig. 5 a, c, e) present more wear evolution than the tests done under water lubrication (fig. 5 b, d, f). Furthermore, in both lubrication conditions, wear increases with the applied load. The increase of wear can be also visualized in Figure 6, where the wear rate is plotted at different loads for dry (fig. 6a) and water lubricated (figure 6b) tests. The topographical evolution of the wear tracks can be studied through their roughness changes, as illustrated in figure 7 with experiments at the three loads for dry (fig. 7a) and water-lubricated (fig. 7b) conditions. Figure 8 shows the CoF, recorded simultaneously with the wear data evolution displayed in figures 5 and 6, and the roughness in figure 7.

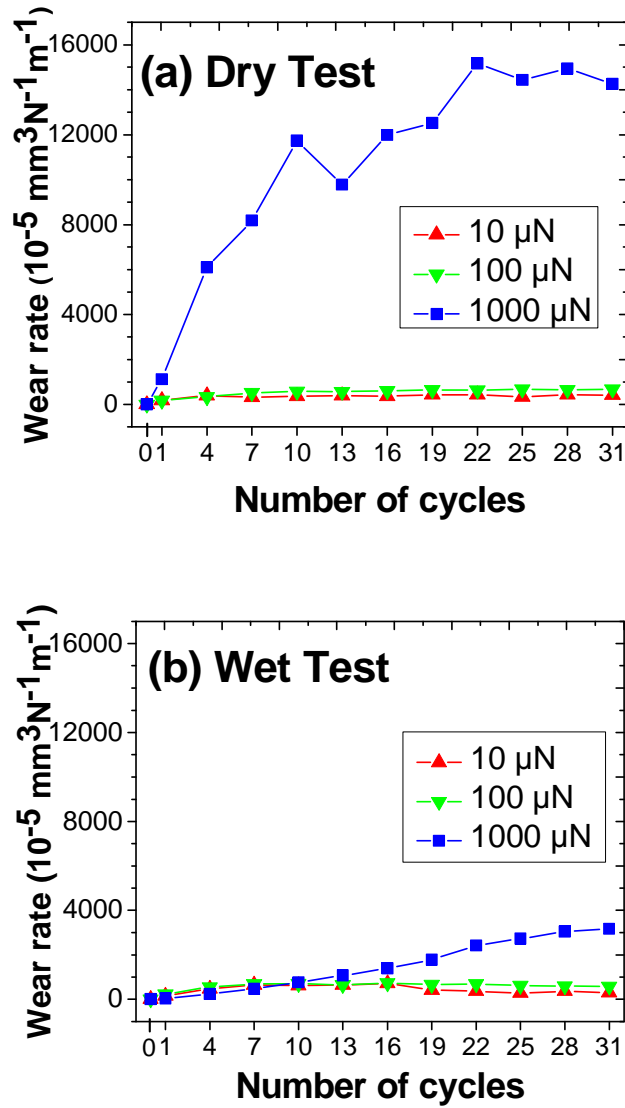


FIG. 6. (Color Online) Wear rate as a function of the number of cycles for (a) dry and (b) water-lubricated tests.

It has been known for centuries that carbon-derived bulk materials, such as graphite, have outstanding lubrication properties. These materials designed for lubricating purposes with low friction coefficient (0.001 to 0.3) and good durability in different environments require understanding their tribological behavior in order to take innovative approaches for

manufacturing applications<sup>9</sup>. Macro-tribological studies on bulk amorphous carbon materials started in the 1950's and 1960's during the development of carbon bearings and seals<sup>10,11</sup>, and later in the

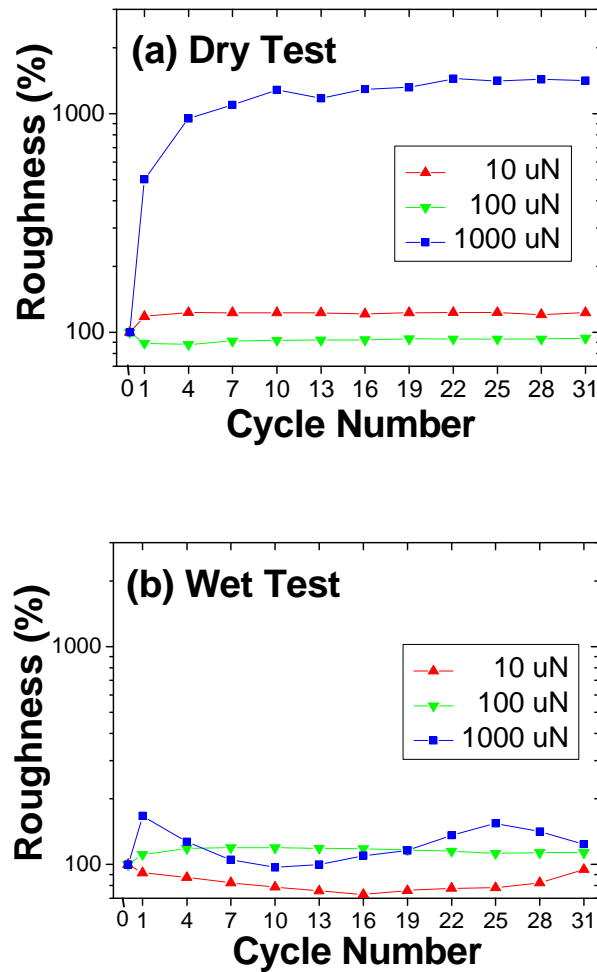


FIG. 7. (Color Online) Roughness as a function of the number of cycles for (a) dry and (b) water-lubricated tests.

1990's to understand environmental effects on friction and wear in the design of disc brakes<sup>12,13</sup>. For studies at the micro- and nano-scale we must, however, relate to studies of



non-hydrogenated diamond-like carbon (DLC) coatings. These amorphous films are a mix of  $sp^3$  tetrahedral bonding (like in single-crystal diamonds) and  $sp^2$  trigonal bonding (like in single-crystal graphite), and usually deposited by physical or chemical vapor deposition techniques<sup>14</sup>. Since Bhushan published the first nanotribological study of amorphous carbon films using an atomic force microscope (AFM)<sup>15</sup>, there have been many studies about the nanotribological properties of carbon-based coatings, as it has been reviewed for dry and lubricated conditions<sup>16-22</sup>.

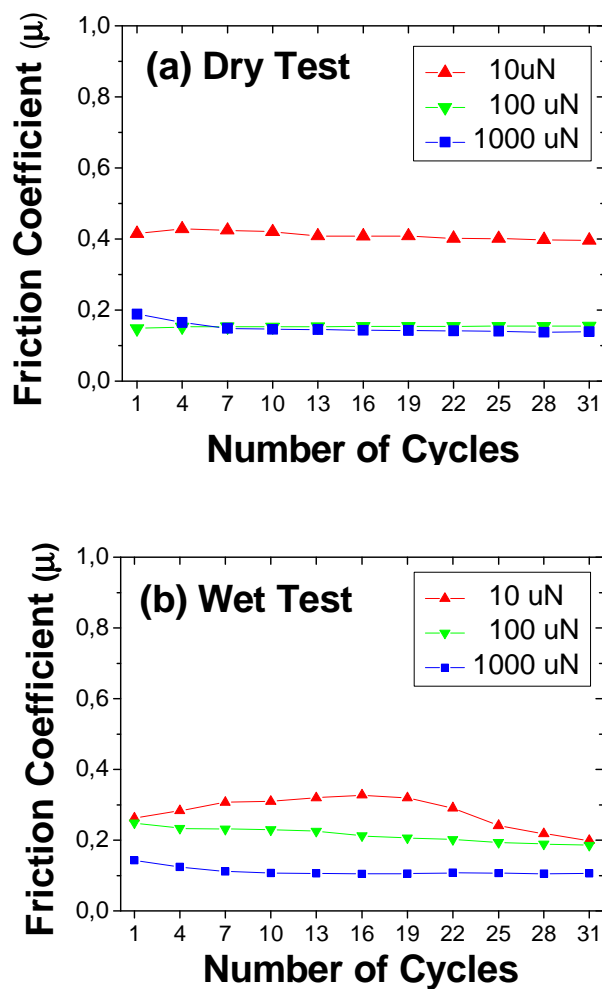


FIG. 8. (Color Online) Friction coefficient as a function of the number of cycles for (a) dry and (b) water-lubricated tests.

We can observe that for dry tests (Figure 8a), the friction coefficient decreases with the increase of the applied load from 10  $\mu\text{N}$  to 100  $\mu\text{N}$ , and stays constant when increasing from 100  $\mu\text{N}$  to 1000  $\mu\text{N}$ . Schiffmann *et al* have shown that the friction coefficient of non-hydrogenated DLC films can be written as

$$\mu = c_1L^{-1/3} + c_2L^m \quad (2)$$

where  $L$  is the applied load, ( $c_1$ ,  $c_2$ ) are constants, and  $m$  is a ploughing exponent in the range 0.7-1.2<sup>7</sup>. The first term is dominant in the case of pure elastic deformation, and the second term represents the ploughing contribution in a plastic deformation regimen. Results from figures 5a, 6a, and 7a support the friction data because there is practically no wear at 10  $\mu\text{N}$  and 100  $\mu\text{N}$ , while at 1000  $\mu\text{N}$  there is wear due to ploughing and plastic deformation.

If we analyze now the  $\mu$  cycle-dependence for dry friction (figure 8a), it is essentially constant over the whole experiment for the lower loads, confirming that the surface is elastically deformed and that there is little or no ploughing. At the highest load of 1000  $\mu\text{N}$ , a CoF drop in the first cycles occurs and then stays constant. The friction behavior correlates with the wear and roughness evolution, which have a big increase during the first 4 cycles while a big trench is built, and then the variation is very small until the end of the experiment.

In the case of water lubrication, at each applied load and cycle, the CoF in water lubrication is always lower than in dry conditions (figure 8). It has been previously shown that water acts as a lubricant for DLC coatings<sup>19, 23</sup>. The lubricating action of the water can be explained as a result of a “three-body interaction” where the water reduces the adhesion between the surfaces in contact. At low loads, the contact pressure is not large enough to squeeze the water molecules from the contact area and, thus, the water plays the role of a

lubricating liquid. On the other hand, at the higher load, the large pressure generated at the contact region squeezes some of the water molecules out of the contact region, and some wear takes place between dry surfaces.

## **V. SUMMARY AND CONCLUSIONS**

We have introduced a new methodology to measure simultaneously the friction and wear of a surface at the nano- and micro-scale. An experiment has been designed with a probe which is permanently scanning a 10  $\mu\text{m}$  track in a reciprocal movement. Different loads are applied in order to obtain the topographic information which is used to calculate the wear rate and roughness evolution, while lateral force sensors acquire the friction force values. The data is processed using a simple program running in MathLab® which eliminates the thermal drift. The software output gives the resulting friction coefficient, track roughness, and wear rate as a function of the running cycles of the probe.

## **ACKNOWLEDGMENTS**

The authors acknowledge the support from the Swedish Government Strategic Research Area Grant in Materials Science at Linköping University (SFO-Mat-LiU) on Advanced Functional Materials. EB acknowledges the partial support from COST Action MP1303 “*Understanding and Controlling Nano and Mesoscale Friction*”. FJFR is grateful with the “Consejo Nacional de Ciencia y Tecnología” (CONACyT) regarding the awarded scholarship for the stage at Linköping University.

## REFERENCES

- <sup>1</sup>M. Urbakh and E. Meyer, "The renaissance of friction," *Nat Mater* **9**, 8 (2010).
- <sup>2</sup>E. Broitman, "The nature of the frictional force at the macro-, micro-, and nano-scales," *Friction* **2**, 40 (2014).
- <sup>3</sup>B. Bhushan and J.-A. Ruan, "Atomic-Scale Friction Measurements Using Friction Force Microscopy: Part II—Application to Magnetic Media," *J Tribol-T ASME* **116**, 389 (1994).
- <sup>4</sup>B. Bhushan, "Nanotribology, nanomechanics, and nanomaterials characterization," *Philos T R Soc A* **366**, 1351 (2008).
- <sup>5</sup>K. I. Schiffmann, "Microtribological/mechanical testing in 0, 1 and 2 dimensions: A comparative study on different materials," *Wear* **265**, 1826 (2008).
- <sup>6</sup>T. W. Scharf and J. A. Barnard, "Nanotribology of ultrathin a:SiC/SiC-N overcoats using a depth sensing nanoindentation multiple sliding technique," *Thin Solid Films* **308–309**, 340 (1997).
- <sup>7</sup>K. I. Schiffmann and A. Hieke, "Analysis of microwear experiments on thin DLC coatings: friction, wear and plastic deformation," *Wear* **254**, 565 (2003).
- <sup>7</sup>"TriboIndenter TI-950," Hysitron, 2015. [Online]. Available: <http://www.hysitron.com/products/ti-series>. [Accessed 10 January 2015].
- <sup>9</sup>K. Miyoshi, S. Takeuchi, M. Suzuki and M. Watanabe, "Solid Lubrication by Novel Carbon-derived Materials," *New Diam Front C Tec* **15**, 37 (2005).
- <sup>10</sup>F. J. Clauss, *Solid Lubricants and Self-Lubricating Solids* (Elsevier, New York, 2012).

- <sup>11</sup>S. Lafon-Placettea, K. Delbé, J. Denape and M. Ferrato, "Tribological characterization of silicon carbide and carbon materials," *J Eur Ceram Soc* **35**, 1147 (2015).
- <sup>12</sup>B. K. Yen, "Influence of water vapor on the tribology of carbon materials with sp<sup>2</sup> valence configuration," *Wear* **192**, 208 (1996).
- <sup>13</sup>C. Blanco, J. Bermejo, H. Marsh and R. Menendez, "Chemical and physical properties of carbon as related to brake performance," *Wear* **213**, 1 (1997).
- <sup>14</sup>E. Broitman and L. Hultman, "Advanced Carbon-based Coatings," in *Comprehensive Materials Processing - Vol. 4 Thin Films* (Elsevier, Amsterdam, 2014) 389–412. .
- <sup>15</sup>B. Bhushan, V. Koinkar and J.-A. Ruan, "Microtribology of magnetic media," *P I Mech Eng J-J Eng* **208**, 17 (1994).
- <sup>16</sup>E. Broitman and L. Hultman, "Tribology of Carbon-based Coatings: Past, Present, and Future," in *Proc. 2nd International Workshop of Tribology Tribaires 2013* (Sociedad Argentina de Tribology, Buenos Aires, 2013) pp. 7-10.
- <sup>17</sup>E. Broitman, Z. Czigány, G. Greczynski, J. Böhlmark, R. Cremer and L. Hultman, "Industrial-scale deposition of highly adherent CN<sub>x</sub> films on steel substrates," *Surf Coat Tech* **204**, 3349 (2010).
- <sup>18</sup>C. A. Charitidis, "Nanomechanical and nanotribological properties of carbon-based thin films: A review," *Int J Refract Met H* **28**, 51 (2010).
- <sup>19</sup>C. A. Charitidis, E. O. Koumoulus and D. A. Dragatogiannis, "Nanotribological Behavior of Carbon Based Thin Films: Friction and Lubricity Mechanisms at the Nanoscale," *Lubricants* **1**, 22 ( 2013).

- <sup>20</sup>B. Bhushan, "Nanotribology of ultrathin and hard amorphous carbon films," in *Tribology of Diamond-Like Carbon Films* (Springer, New York, 2008) 510-570.
- <sup>21</sup>D. S. Grierson and R. W. Carpick, "Nanotribology of carbon-based materials," *Nanotoday* **2**, 12 (2007).
- <sup>22</sup>F. J. Flores-Ruiz, C. I. Enriquez-Flores, F. Chinas-Castillo and F. J. Espinoza-Beltrán, "Nanotribological performance of fullerene-like carbon nitride films," *Appl Surf Sci* **314**, 193 (2014).
- <sup>23</sup>E. Broitman, W. Macdonald, N. Hellgren, G. Radnóczy, Z. Czigány, A. Wennerberg, M. Jacobsson and L. Hultman, "Carbon nitride films on orthopedic substrates," *Diam Relat Mater* **9**, 1984 (2000).
- <sup>24</sup>L. Sirghi, V. Tiron and M. Dobromir, "Friction at single-asperity contacts between hydrogen-free diamond-like carbon thin film surfaces," *Diam Relat Mater* **52**, 38 (2015).
- <sup>25</sup>E. Broitman and L. Hultman, "Adhesion Improvement of Carbon-based Coatings through a High Ionization Deposition Technique," *J Phys Conf Ser* **370**, 012009 (2012).